Riv. It. Paleont. Strat.	v. 100	n. 2	pp. 307-322	tav. 1-3	Ottobre 1994

DOLOMITIC SEDIMENTS IN CORE BAN 89-22 GC FROM THE DEEP-SEATED BRINES OF BANNOCK BASIN, EASTERN MEDITERRANEAN

SIBIANA ONETO, MARIA CARLA SALA & MARIA BIANCA CITA

Key-words: Eastern Mediterranean, Dolomitic sediments, Brine lake.

Riassunto. La carota BAN 89-22 GC è stata prelevata nel Bacino Bannock (Mediterraneo Orientale) sulla larga soglia che separa i sub-bacini Maestro e Borea in un'area ricoperta da salamoie ad alta densità. L'interesse di questa carota consiste nella sua composizione dolomitica. Per questa ragione è stato svolto uno studio dettagliato utilizzando tecniche particolari (T.A.C., percentuale in carbonati utilizzando HCl al 5% e 17%, osservazione di smear-slides per ogni campione sia per la datazione tramite nannofossili calcarei sia per lo studio della composizione mineralogica della frazione siltosa di sedimento, EDAX), che hanno consentito di attribuire a diagenesi secondaria la composizione dolomitica dei sedimenti. Tale diagenizzazione sarebbe dovuta a migrazione verso l'alto per diffusione o per avvezione di ioni Mg^{++} provenienti dalla dissoluzione di dolomite primaria del Messiniano.

Abstract. Core Ban 89-22 GC has been recovered in the Bannock Basin (Eastern Mediterranean) on the large sill separating Borea and Maestro sub-basins in an area covered by high density brines. The interest of this core consists in its dolomitic composition, for this reason the core has been studied in its sedimentological and micropaleontological characters with great detail. The use of particular analyses (C.A.T. Computerized axial tomography, carbonate percentage, smear-slides observations of all samples for the identification of nannofossil Zones and for the mineralogic composition of the sediments, EDAX) allows to explain the dolomitic composition as secondary diagenization due to the upward molecular diffusion or advection of Mg^{++} ions from the dissolution of primary dolomite of Messinian age, recovered in the core-catcher thus in contact with the Pleistocene-Holocene core sediments.

Introduction.

The Bannock Basin, discovered in 1984, is located on the southern flank of the Mediterranean Ridge, at 34°20' lat N and 20°00' long E (Cita et al., 1986). The basin is a large deep subcircular depression composed of nine sub-basins aligned along a rim-syncline surrounding a central dome-like area (Fig. 1). It reaches water depth of 3540 m in Libeccio Basin (Camerlenghi & McCoy, 1989). The entire area of the de-

- Dipartimento di Scienze della Terra dell'Università degli Studi di Milano, via Mangiagalli 34, 20133 Milano, Italy.

pression, delimited by the first closed isobath, is 214 km^2. Brines with density about 1.2 g/cm^3 and salinity about ten times more than the normal sea water fill the basin and cover an area of about 46.5 km^2.

The brine origin is attributed to the dissolution of the Messianian evaporites which can be found about 200 m below the seafloor. The evaporites are supposed to outcrop on the steep (50°-80°) inner slope of the basin (Camerlenghi & Cita, 1987).

The brines are separated from the normal sea water by a sharp interface, at -3200 m. Below this depth a sharp increase occurs for electrical conductivity (salinity); the temperature of the brines is higher than normal bottom water (Rabitti & Boldrin, 1989; De Lange et al., 1990a; De Lange et al., 1990b; De Lange et al., 1990c).

Sediments deposited in the anoxic brines are characterized by (Montagnana & Sala, 1993): dark colour; occurrence of a thinly laminated sedimentary facies, and a non-laminated facies containing thin turbidites and/or debris flows; presence of a Holocene homogeneous pelagic turbidite dated 3500 yr B.P.; absence of bioturbations;

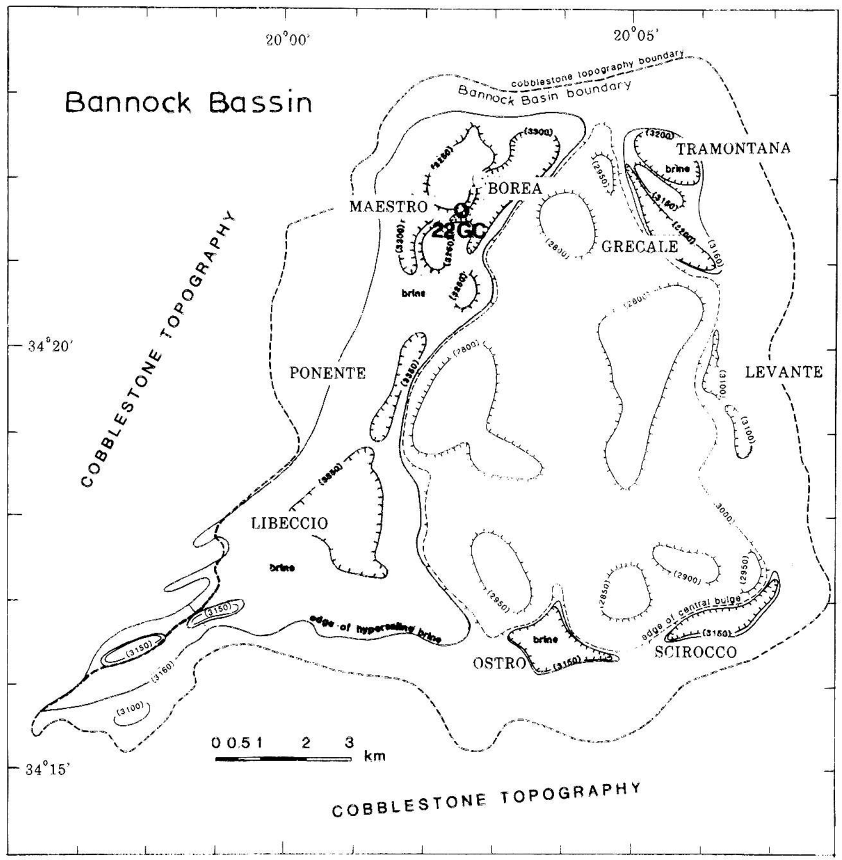

Fig. 1 - Simplified bathymetry of Bannock Basin. Location of the core BAN 89-22 GC.

fine grained texture; biogenic fraction including siliceous plankton (Björklund & De Ruiter, 1987); terrigenous fraction mostly fine-grained; occurrence of authigenic minerals such as gypsum and pyrite. Moreover, inside these sediments, bacterial pellicles are present (Erba et al., 1987; Erba, 1991).

Purpose of the present work is to present the results of a very detailed study of a short (106 cm long) dolomite-bearing core raised from the sill separating the Maestro and Borea sub-basins, below the brine, where barren dolomitic mudstone attributed to the Messinian were recovered in the core-catcher (Cita & Aghib, 1991).

Materials and methods.

The study is based on core Ban 89-22 GC (Fig. 1), located at 34°21.88' lat N and 20°02.34' long E at 3229 m water depth. An unusually high pull-out tension was measured, during extraction of the gravity corer from the seafloor (>6 t), and solid rocks were recovered (see below).

The core was not immediately opened after its recovery (only the core-catcher was analyzed) because it was planned to run XR analysis and to measure sediment density which requires intact material. C.A.T. (Computerized Axial Tomography) in transversal and longitudinal section was executed on the core and the trigger in order to identify the sedimentological structures present (courtesy of the S. Raffaele Hospital in Milano).

The core was then opened on April 22, 1992: it was photographed, visually described, and sampled. Three samples were analyzed for bulk density in the Geotechnical Laboratory of the Department of the Earth Science (Milano University). On the remaining twenty-two samples the following analyses have been carried out: a) colour determination, b) smear-slides for semiquantitative evaluation of the mineralogical and micropaleontological contents, c) identification of the nannofossils Zones, d) carbonate content, using HCl at 5% and 17% on a Dieter Freeling calcimeter to monitor the possible presence of dolomite, e) texture observations at S.E.M., f) compositional study by EDAX microprobe, g) compositional and micropaleontological study of sand fraction wet sieved and weighted.

Sediments composition.

Two lithologies were identified in the core-catcher. The first is an olive-grey dolomitic-mudstone (Cita & Aghib, 1991), similar to others found in eastern Mediterranean: a) in the Aphrodite Crater, in Cobblestone Area 3 (Blechschmidt at al., 1982), b) in the Messina Abyssal Plain (DSDP Site 374) (see Hsü, Montadert et al., 1978), and c) on the flank of Victor Hensen Seahill (Cruise Report BAN-81, 1981 unpublished).

The second lithology is a real rock with lithic consistency which could partly explain the exceptional "pull-out" registered during its recovery. It is saccharoidal dolomite characterized by millimetric sub-spherical cavities (Cita & Aghib, 1991).

Both lithologies are entirely devoid of micro- and nannofossils, and they have been tentatively attributed to the Messinian. They could be part of the "cap rock" of a dome in the rising phase, or part of the Upper Messinian evaporites collapsed in the rim-syncline. This second hypothesis is in accordance with the relief inversion characterizing the Mediterranean Ridge (Camerlenghi & Cita, 1987) and in particular with the discovery of sediments from Early Pliocene age (Biozone MPl2) in BAN 88-17 core (Levante-Scirocco sill) (Cita, 1989; Cita & Aghib, 1991).

Two different sediment types were identified inside the main core: the first, present from the top down to 34 cm and from 38 to 80 cm, includes dark silty mud typical of Bannock Basin containing an extrabasinal turbidite possibly of North African origin; the second (from 34 to 38 cm and from 80 to 106 cm), is composed by dolomitic mudstone.

I) The normal anoxic sediments.

From the top to 10 cm, the sediment consists of homogeneous grey mud with abundant carbonate components (Tab. 1) and carbonate percentage around 30% (Fig. 2). The sand constitutes only 3.1% in weight of the total sediment. The fraction over 151 μm consists of planktonic and very few benthonic foraminifers, radiolaria and pteropods: filamentous organic matter incorporating foraminifers and radiolaria is present.

From 10 to 34 cm from core top the sediment consists of olive-grey gelatinous mud rich in organic pellicles and gypsum crystals also in centimetric size. Smear-slides

BAN 89–22 GC																	
cm from top			Biogenic								Non biogenic						
	Tot. non bio.	Tot. bio.	Calcareous				Siliceous										
			foram.	nanno.	thoraco.	spic.	rad.	diat.	silico.	spic.	Qz	feld.	micas	ossides	calc.	pyrite f.	dolom.	gyps.
4.5–5.5	a	a	c	a	Tr	Tr	R	Tr	Tr	Tr	Tr	Tr	Tr	Tr	c	c	R	Tr
10–11	c	A	c	a	R	Tr	c	c	Tr	Tr	Tr	Tr	Tr	Tr	c	c	R	R
14.5–15.5	a	a	R	C	Tr	Tr	c	c	R	Tr	Tr	Tr	Tr	Tr	c	c	R	R
20–21	a	a	R	C	Tr	Tr	c	c	R	Tr	Tr	Tr	Tr	Tr	c	c	R	R
25–26	a	a	R	C	Tr	Tr	c	c	R	Tr	Tr	Tr	Tr	Tr	c	c	R	R
29–30	A	c	R	C	Tr	Tr	C	Tr	Tr	Tr	R	Tr	Tr	Tr	c	c	R	R
31.5–32.5	A	c	R	C	Tr	Tr	C	Tr	Tr	Tr	R	Tr	Tr	Tr	c	c	R	R
36.5–37.5	D	Tr	Tr	Tr	Tr	Tr	Tr	Tr	Tr	Tr	Tr	Tr	Tr	Tr	Tr	Tr	D	c
40–41	a	a	R	C	R	Tr	C	c	Tr	Tr	Tr	Tr	Tr	Tr	Tr	c	R	R
45–46	a	a	R	a	Tr	Tr	R	c	Tr	Tr	Tr	Tr	Tr	Tr	Tr	Tr	R	R
50–51	a	a	C	a	Tr	Tr	R	R	Tr	Tr	R	Tr	Tr	Tr	Tr	Tr	R	R
55–56	a	a	a	c	Tr	Tr	–	–	–	Tr	R	Tr	Tr	Tr	Tr	Tr	R	R
59–60	a	a	c	a	Tr	Tr	–	–	–	Tr	R	Tr	Tr	Tr	Tr	Tr	R	Tr
65–66	a	a	c	C	Tr	Tr	Tr	–	–	Tr	R	Tr	Tr	Tr	Tr	Tr	R	R
70–71	a	a	C	C	Tr	Tr	–	–	–	Tr	R	Tr	Tr	Tr	Tr	Tr	R	R
75–76	a	a	C	C	Tr	Tr	–	–	–	Tr	R	–	Tr	Tr	Tr	Tr	R	R
80–81	D	Tr	–	–	–	–	–	–	–	–	Tr	–	–	–	Tr	Tr	D	Tr
86.5–87.5	D	Tr	Tr	Tr	–	–	–	–	–	–	–	–	Tr	Tr	Tr	Tr	D	Tr
89–90	D	Tr	–	–	–	–	–	–	–	–	–	–	Tr	Tr	Tr	Tr	D	Tr
93.5–94.5	D	Tr	–	Tr	–	–	–	–	–	–	Tr	–	Tr	Tr	Tr	Tr	D	Tr
102–103	D	Tr	–	Tr	–	–	–	–	–	–	Tr	–	Tr	Tr	Tr	Tr	D	Tr
104.5–105.5	D	Tr	–	Tr	–	–	–	–	–	–	Tr	–	Tr	Tr	Tr	Tr	D	Tr

D = dominant (>75%) A = abundant (75–50%) a = abundant (50–30%)
c = common (15–5%) R = rare (5–1%) Tr = trace
C = common (30–15%)

Tab. 1 - Results of smear-slides observation.

show that in the biogenic component the siliceous prevails, with abundance of organic matter and framboidal pyrite as previously noticed in the other cores coming from Bannock Basin (Parisi et al., 1987; Montagnana & Sala, 1993). The decrease in carbonate biogenic component is confirmed by a decrease in carbonates (average 26%). The same decrease is shown by the sand fraction (avg 2.9% in weight on total sediment). The fraction over 151 μm appears to be composed by planktonic foraminifers (Tab. 2) and radiolaria. The benthonic foraminifers (Tab. 3) are rare to absent: pteropods (Tab. 4) are present with protoconchs, entire specimens and fragments. The organic matter is abundant: under filamentous form, amber colored laminas, and as organic pellicles. Tests of partially or totally dolomitized or pyritized foraminifers are present (Pl. 1).

From 34 to 50 cm the sediment consists of laminated mud with sub-parallel laminations of different thickness and colour, detectable by visual observation and on C.A.T. in longitudinal section (Fig. 2). At 40-41 cm there is a gelatinous layer of organic pellicles, whose presence is pointed out by a negative peak of the carbonate curve (14%) as it has already been underlined in previous studies (Montagnana & Sala, 1993). The residue over 151 μm (0.3% in weight) shows abundant organic pellicles incorporating planktonic foraminifers and radiolaria. Benthonic foraminifers and pteropods are absent. Between 41 and 50 cm the carbonate content (21.3%) is lower than in the previously considered interval (10-34 cm): such decrease is also evident from the observation of smear-slides where the prevalence of siliceous biogenic component over the carbonatic is noticed. The fraction of the sediment over 151 μm represents 2.5% of total weight, a figure similar to the previous interval. However, a trend to increase downward of the percentage in weight of the fraction over 151 μm with a parallel decrease of the fraction between 60 μm and 151 μm is noticed in this

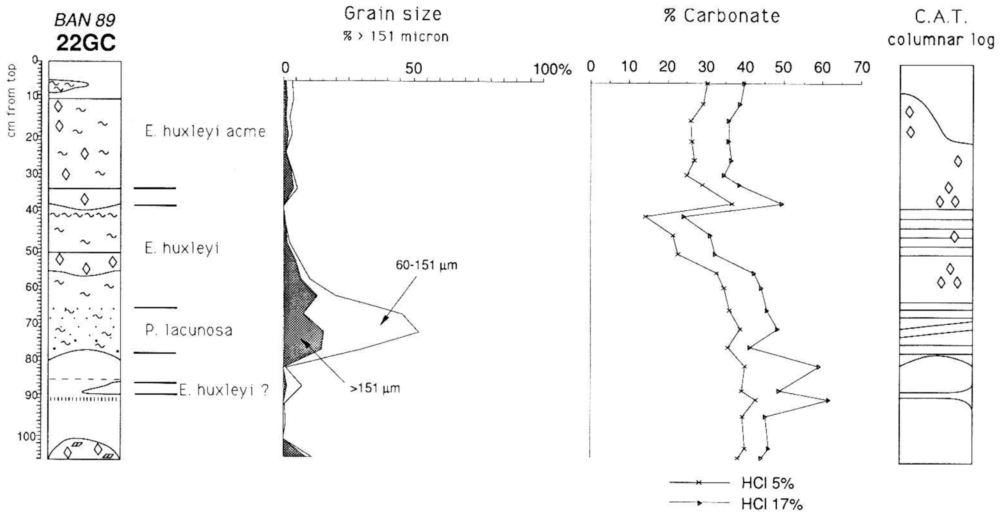

Fig. 2 - Nannofossil zones, grain size, carbonate percentages and C.A.T. columnar log of BAN 89-22 GC.

BAN 89–22 GC

cm from top	Planktonic foraminifers																																				
	G. ampliapertura	G. apertura	G. bulloides	G. calida	G. cariacoensis	G. ciperoensis	G. digitata	G. glutinata	G. praecalida	G. praedigitata	G. quinqueloba	Gs. conglobatus	Gs. elongatus	Gs. fistulosus	Gs. gomitulus	Gs. helicinus	Gs. pyramidalis	Gs. ruber	Gs. ruber pyramidalis	Gs. sacculifer	Gs. tenellus	Gs. trilobus	Gr. anfracta	Gr. crassaformis	Gr. hirsuta	Gr. inflata	Gr. margaritae	Gr. oscitans	Gr. scitula	Gr. tosaensis	T. truncatulinoides	T. truncatulinoides pachyteca	N. eggeri dutertrei	N. pachyderma	O. bilobata	O. universa	H. siphonifera	S. dehiscens
4.5–5.5			x	x	x			x		x		x	x		x	x	x	x		x	x	x	x			x		x	x		x		x			x	x	
10–11			x	x						x		x	x			x	x	x	x	x		x	x			x			x		x		x	x		x	x	x
14.5–15.5			x							x		x	x			x	x	x	x	x		x	x		x	x		x			x		x	x	x	x	x	x
20–21										x		x	x			x	x	x	x	x		x				x		x	x		x		x	x			x	
25–26			x	x				x				x	x					x		x		x				x			x		x		x	x	x	x		
29–30			x					x	x	x																x		x	x	x	x	x	x	x		x	x	
31.5–32.5			x			x		x	x		x	x	x							x		x	x			x			x		x		x	x	x	x	x	
36.5–37.5						x		x		x								x																		x		
40–41			x		x			x				x	x		x			x				x				x		x	x		x		x	x		x	x	
45–46			x		x			x							x	x		x	x							x			x				x	x		x		
50–51			x	x	x			x		x			x	x	x		x	x	x							x		x	x				x	x		x	x	
55–56			x	x	x					x		x	x		x	x		x		x		x				x		x	x		x		x	x		x	x	
59–60	x		x									x	x		x		x	x	x	x		x				x			x		x		x	x	x	x	x	
65–66			x	x			x	x		x	x	x	x		x			x	x	x	x	x		x		x		x	x		x		x	x		x	x	
70–71			x	x						x	x	x	x		x		x	x	x	x	x					x			x		x		x	x	x	x	x	x
75–76			x	x				x		x	x	x	x				x	x						x		x	x		x		x		x		x	x	x	
80–81																		x																x				
86.5–87.5							x	x		x			x		x	x	x				x	x				x			x		x		x		x	x	x	
89–90			x	x								x	x		x			x				x				x			x		x		x	x		x		
93.5–94.5			x										x		x			x			x					x					x		x	x		x		
102–103			x	x				x							x			x								x										x		
104.5–105.5			x					x		x					x			x								x			x				x	x		x		

G. = Globigerina, Gs. = Globigerinoides, Gr. = Globorotalia

Tab. 2 - Planktonic foraminifers identified in BAN 89-22 GC core.

layer. In the 151 μm residue planktonic foraminifers (Tab. 2) sometimes with dolomitized and/or pyritized tests, radiolaria and plenty of organic matter are present, whereas benthonic foraminifers and pteropods are absent. In this interval sub-spherical structures (about 200 μm diameter) or deformed (Pl. 1), transparent and traslucent, yellow dark colour, isolated or in chains, of probable biogenic origin were observed. EDAX analysis on these spherical bodies did not show the presence of inorganic components. The size and the absence of ornamentations on the wall suggests they are eggs of gastropods (Pl. 1, fig. 4).

In the next interval, from 50 to 80 cm a transition between grey-olive mud with gelatinous consistency to dark grey sand is recorded. The fraction of the sediment over 60 μm between 50 and 60 cm averages 12% on the total weight (over 151 μm avg 8.1%), whilst from 61 to 80 cm it reaches very high values (avg 42%, maximum value

BAN 89–22 GC

cm from top	Benthonic foraminifers																																																																			
	Angulogerina angulosa	Anomalina sp.	Anomalinoides sp.	Anomalinoides helicinus	Anomalinoides minimus	Articulina tubulosa	Astaculus crepidulus	Astigerinata planorbis	Biloculinella labiata	Brizalina alata	Brizalina spatulata	Bulimina aculeata	Bulimina costata	Bulimina elegans	Bulimina marginata	Cancris oblongus	Cassidulina carinata	Cassidulina crassa	Cassidulina laevigata	Chilostomella oolina	Cibicides floridanus	Cibicides pseudoungerianus	Cornuspira sp.	Discorbinella biconcava	Ellipsopolymorphina fragilis	Elphidium advenum	Elphidium sp.	Eponides tenerus	Fissurina cucullata	Fissurina pseudorbignyana	Fissurina submarginata	Fursenkoina sp.	Gyroidina neosoldanii	Gyroidinoides laevigatus	Gyroidinoides longispira	Glandulina laevigata	Globobulimina sp.	Globobulimina pseudospinescens	Heterolepa mexicana	Lagena sp.	Lenticulina gibba	Lenticulina sp.	Melonis padanum	Melonis pompilioides	Melonis soldanii	Nodosaria scalaris	Nonionella sp.	Oolina exagona	Oridorsalis westi	Parafissurina sp.	Planulina ariminensis	Protelphidium sp.	Pullenia compressiuscula	Pullenia quinqueloba	Pyrgo oblonga	Rosalina bradyi	Rosalina globularis	Reussella sp.	Reussella spinulosa	Sigmoilina tenuis	Siphonina reticulata	Siphonodosaria sp.	Textularia sp.	Uvigerina cushmani	Uvigerina mediterranea	Uvigerina peregrina	Uvigerina sp.	Valvulineria complanata	Verneuilina tricarinata
4.5–5.5																							X		X							X																																					
10–11																																																																					
14.5–15.5									X																																																												
20–21																																																																					
25–26																																																																					
29–30																																																									X									
31.5–32.5																																																																					
36.5–37.5																																																																					
40–41																																																																					
45–46																																																																					
50–51										X																																																												
55–56																									X																																												
59–60		X				X																																								X																							
65–66					X	X				X		X	X		X	X		X	X	X									X				X									X				X				X			X	X		X	X	X			X			X	X		X		
70–71	X		X					X		X		X	X					X		X	X				X		X	X	X	X	X	X	X	X	X	X	X		X			X		X	X		X	X	X			X		X	X	X						X	X		X		X	X	X
75–76	X	X	X	X			X			X	X	X	X	X	X		X			X		X		X		X		X	X									X		X	X		X		X	X		X	X		X					X			X						X	X	X		
80–81											X																																																					X				
86.5–87.5	X									X							X					X																													X																		
89–90						X																																																															
93.5–94.5																																												X																									
102–103																																																																					
104.5–105.5																																																																					

Tab. 3 - Benthonic foraminifers identified in BAN 89-22 GC core.

BAN 89–22 GC

cm from top	Pteropods										
	Atinta fusca	Atlanta helicinoides	Clio pyramidata	Creisis aciculata	Diacria trispinosa	Firoloida desmaresti	Gleba cordata	Limacina inflata	Limacina trochiformis	Styliola subrotunda	Styliola subula
4.5–5.5	X	X	X	X	X	X	X	X	X	X	X
10–11		X		X				X			X
14.5–15.5	X				X						
20–21	X		X				X			X	X
25–26	X		X	X		X		X			X
29–30											
31.5–32.5		X	X		X	X		X	X		
36.5–37.5											
40–41											
45–46											
50–51											
55–56											
59–60											
65–66											
70–71											
75–76											
80–81											
86.5–87.5											
89–90											
93.5–94.5											
102–103											
104.5–105.5											

Tab. 4 - Pteropods identified in BAN 89-22 GC core.

52% at 70-71 cm). The residue greater than 151 μm consists almost exclusively of planktonic foraminifers, very few radiolaria, organic matter and fragments of pteropods. The same composition is shown by the smear-slides (silty sediment fraction) (Tab. 1). The carbonate percentage is on the average around 33.3% and shows a regular increase from 50 to 80 cm. The interval 60-80 cm contains in abundance benthonic foraminifers (Tab. 3) and (in the residue comprised between 60 μm and 151 μm) clear quartz crystals. This interval, with a coarse, sandy basal part for the presence of benthonic foraminifers indicative of shelf environment such as *Uvigerina, Nonionella, Cibicides* and *Bulimina*, and for the abundance of quartz crystals, is interpretated as an extrabasinal turbidite. Cross laminations in C.A.T. longitudinal section are observed, and support the interpretation of the deposit as a turbidite (Pl. 3).

The non-biogenic component observed in the fraction of sediment below 3 μm, from the top of the core down to 80 cm (35-38 cm interval excluded), is constant. Feldspars, mica, calcite, gypsum, quartz are present, always in trace, exception for the interval between 50-80 cm. Dolomite is present both as single rhombohedral crystals, sometimes zoned with a small portion of micrite in the centre, and as dolomitized tests.

II) Dolomitic sediments.

The second sediment type is present from 34 to 38 cm and from 80 to about 106 cm. The sediment consists almost exclusively of single crystals or small crystalline aggregates of dolomite. Planktonic foraminifers whose tests appear partially or totally dolomitized are quite rare. The percentage of carbonate is 38.5% on the average, with remarkable difference (between 80 and 90 cm) among the percentage obtained after treating the sediment with HCl at 5% and 17%, difference due to dolomite abundance. The parallelism between the two records (HCl 5% and 17%) between 35 and 38 cm could be explained by the presence of Mg-calcite as well as dolomite. The presence both of dolomite and of Mg-calcite has been shown by EDAX analysis.

Two intervals 86.5-87.5 cm and 104.5-105.5 cm (86-87 cm and 104-106 cm C.A.T. images) show an increase in grain size, due to the presence of planktonic foraminifers, uncommon benthonic foraminifers and crystalline aggregates of dolomite. From the second interval, the increase in grain size is due to the presence of dolomitic crystalline aggregates with lithic consistency (same lithology recorded in the core-catcher, see Pl. 2).

Bulk density.

The specific gravity has been measured on three samples at 16.48 and 97 cm and averages 2.493±0.02. This value is lower than the one measured (2.628) for the common hemipelagic sediments of the Eastern Mediterranean (Camerlenghi, 1991).

Sediments age.

Sediments age has been determinated by D. Castradori (pers. comm.). The nannofossil zones identified in the core are reported in Fig. 2.

The calcareous nannofossils indicate an anomalous stratigraphic succession: indeed sediments from the core top to 10 cm, and between 34 to approx. 65 cm are of Late Pleistocene-Holocene age (*E. huxleyi* acme - *E. huxleyi* Zones), while the sediments interpreted as an extrabasinal turbidite (65-80 cm) belong to the Early Pleistocene (*P. lacunosa* Zone) age. These older fossils should be reworked.

Calcareous nannofossils are absent or not age diagnostic in the intervals 34-38 cm and 86.5-106 cm. Strong diagenesis is noticed.

Concluding remarks.

The occurrence of dolomitic sediments in the eastern Mediterranean deep-sea record is fairly well documented (Ryan, Hsü et al., 1973; Hsü, Montadert et al., 1978; Mc Duff et al., 1978; Blechschmidt et al., 1982; De Lange et al., 1990b; Cita & Aghib, 1991). Of special interest is the sedimentary succession penetrated at DSDP Site 374, in the center of the Messina abyssal plain. Here the hemipelagic sediments of Pliocene-

Pleistocene age (Unit 1) are underlain by a thin dolomitic mudstone of diagenetic origin (Unit II), followed downhole by homogeneous dark grey dolomitic mudstone (Unit III, subunit IIIa) of upper Messinian age. A diagenetic origin of the dolomitic sediments of Unit II is attributed to upward migration of Mg^{++} ions deriving by the primary dolomite of Messinian age caused by molecular diffusion or advection (Mc Duff et al., 1978). The above mentioned authors, when studying the chemistry of the interstitial water of post-Messinian sediments recovered in the Mediterranean, showed that the presence of Messinian evaporites underlying the sediments exerts a strong influence in the chemical composition of the pore solutions, and recorded gradients compatible with the diffusion model.

The sedimentary succession recorded in our short core resembles to that of DSDP Site 374, with hemipelagic sediments (and re-sediments) followed by diagenetic dolomitic mudstones containing, near the base, centimetric little masses of saccharoidal dolomite. The occurrence of dolomitized tests of foraminifers and of diagenetically overgrown coccolitophorids allows to exclude a Messinian age for these dolomitic sediments, since Messinian dolomites are notoriously barren. Finally, the barren dolomitic mudstone in the core-catcher are interpreted as primary Messinian dolomites. Following Mc Duff et al. (1978) we attribute the dolomitic diagenesis to upward migration of Mg^{++} ions by molecular diffusion.

The occurrence of a thin dolomitic interval (from 34 to 38 cm from top core) within the hemipelagic sediments is intriguing: it might be a coring artifact (double penetration of the gravity corer in the subbottom) or, more likely, be due to submarine slumping.

The strongly condensed nature of the core agrees well with the inversion of relief characterizing the collapsed, partly brine-filled basins of the Mediterranean Ridge accretionary complex (Camerlenghi & Cita, 1987; Cita & Aghib, 1991).

Acknowledgments.

We gratefully acknowledge E. Erba, S. Frisia and R. Sanvoisin for discussing various aspects of this study. We also would like to thank dott. G. Crespi of the Diagnostic Radiology Department - S. Raffaele Hospital - for the interest shown in our research; L. Magni for bulk density analysis; A. Rizzi and G. Chiodi for photographical assistance. The accurate revisions provided by G. De Lange and A. Camerlenghi contributed to improve the present text.

This research was supported by a grant MURST 40% to M.B. Cita.

REFERENCES

Björklund K. R. & De Ruiter R. (1987) - Radiolarian preservation in Eastern Mediterranean anoxic sediments. *Mar. Geol.*, n. 75, pp. 271-281, Amsterdam.

Blechschmidt G., Cita M. B., Mazzei R. & Salvatorini G. (1982) - Mediterranean and south Calabrian Ridge, Eastern Mediterranean. *Mar. Micropleont.*, v. 7, pp. 101-134, Amsterdam.

Camerlenghi A. & Cita M. B. (1987) - Setting and tectonic evolution of some Eastern Mediterranean deep-sea basins. *Mar. Geol.*, n. 75, pp. 31-53, Amsterdam.

Camerlenghi A. & McCoy F. W. (1989) - Bathymetry, morphology and structure of Bannock Basin. Anoxic Basins of the Eastern Mediterranean. *Ric. Sc. Ed. Perm.*, suppl. 72, pp. 9-11, Milano.

Camerlenghi A. (1991) - Il diapirismo d'argilla sulla Dorsale Mediterranea. Tesi di dottorato, Univ. degli Studi di Milano, pp. 94-98, Milano.

Cita M. B. (1989) - Evidence of relief inversion in satellite basins (rim-syncline) of Bannock Basin. First results of the BAN 88 cruise. *Ric. Sc. Ed. Perm.*, suppl. 72, pp. 16-17, Milano.

Cita M. B. & Aghib S. F. (1991) - Evidence of relief inversion from the rim-syncline of Bannock Basin. *Mar. Geol.*, n. 100, pp. 67-81, Amsterdam.

Cita M. B., Fornaciari M., Camerlenghi A., Corselli C., Erba E., McCoy F. W. & Vezzoli L. (1986) - Anoxic basins of the Eastern Mediterranean: new evidence from the Bannock Basin area. *Mem. Soc. Geol. Ital.*, v. 36, pp. 131-144, Roma.

De Lange G. J., Middelburg J. J., Van der Weijden C. H., Catalano G., Luther III G. W., Hydes D. J., Wottiez J. R. W. & Klinkhammer G. P. (1990 a) - Composition of anoxic hypersaline brines in the Tyro and Bannock Basins, Eastern Mediterranean. *Mar. Chem.*, v. 31, pp. 63-88, Amsterdam.

De Lange G. J., Boelrjik N. A. I. M., Catalano G., Corselli G., Klinkhammer G. P., Middelburg J. J., Ullman W. J., Van Gaans P. & Wottiez J. R. W. (1990 b) - Sulphate-related equilibria in the hypersaline brines of Tyro and Bannock Basins, Eastern Mediterranean. *Mar. Chem.*, v. 31, pp. 89-112, Amsterdam.

De Lange G. J., Catalano G., Klinkhammer G. P., & Luther III G. W. (1990 c) - The interface between oxic sea-water and anoxic Bannock brines; its sharpness and consequence for the redox-related cycling of Mn and Ba. *Mar. Chem.*, v. 31, pp. 205-217, Amsterdam.

Erba E. (1991) - Deep mid-water bacterial mats from anoxic basins of the Eastern Mediterranean. *Mar. Geol.*, n. 100, pp. 83-101, Amsterdam.

Erba E., Rodondi G., Parisi E., Ten Haven H. L., Nip M. & De Leeuw (1987) - Gelatinous pellicles in deep anoxic basins from Eastern Mediterranean. *Mar. Geol.*, n. 75, pp. 165-183, Amsterdam.

Hsü K. J., Montadert L. et al. (1978) - Initial Reports of the Deep Sea Drilling Project, v. 42, Pt. 1, pp. 1-1244, U.S. Gov. Print. Office, Washington, D.C.

Mc Duff R. E., Gieskes J. M. & Lawrence J. R. (1978) - Interstitial water studies, Leg 42 A. *Init. Repts. DSDP*, v. 42, Pt. 1, pp. 561-568, U.S. Gov. Print. Office, Washington, D.C.

Montagnana S. & Sala M. C. (1993) - La sedimentazione nell'ambiente anossico del Bacino Bannock (Mediterraneo Orientale): caratterizzazione chimica, fisica e biologica dei sedimenti. *Rend. Fis. Acc. Lincei*, s. 9, v. 4, pp. 213-236, Roma.

Parisi E., Erba E. & Cita M. B. (1987) - Stratigraphy and sedimentation in the anoxic Bannock Basin (Eastern Mediterranean). *Mar. Geol.*, n. 75, pp. 93-117, Amsterdam.

Rabitti S. & Boldrin L. (1989) - Vertical structure of temperature, conductivity and trasmittance in Eastern Mediterranean anoxic basins. *Ric. Sc. Ed. Perm.*, suppl. 72, pp. 67-69, Milano.

Ryan W. B. F., Hsü K. J. et al. (1973) - Initial Reports of the Deep Sea Drilling Project, v. 13, pp. 1-1447, U.S. Gov. Print. Office, Washington, D.C.

Received January 29, 1994; accepted June 24, 1994

PLATE 1

Fig. 1a - Foraminiferal test partially dolomitized (core BAN 89-22 CG, sample cm 14.5-15.5).
Fig. 1b - Detail of dolomitized test of fig. 1a.
Fig. 2a - Foraminiferal test entirely dolomitized (core BAN 89-22 GC, sample cm 104,5-105,5).
Fig. 2b - Detail of dolomitized test of fig. 2a.
Fig. 3 - Pyritized foraminiferal test (core BAN 89-22 GC, sample cm 55-56).
Fig. 4 - Probable gastropod eggs (core BAN 89-22 GC, sample cm 45-46).

PLATE 2

Texture and ultratexture of dolomites (core BAN 89-22 GC, sample 102-103 cm).
Fig. 1 - Specimen of dolomite.
Fig. 2, 3 - Cavities of varying sharpe and size.
Fig. 4 - Matrix composed of rhombohedral crystals of dolomite.

PLATE 3

C.A.T. images of BAN 89-22 GC core. Above: longitudinal sections; below: cross sections (3 and 6 cm).

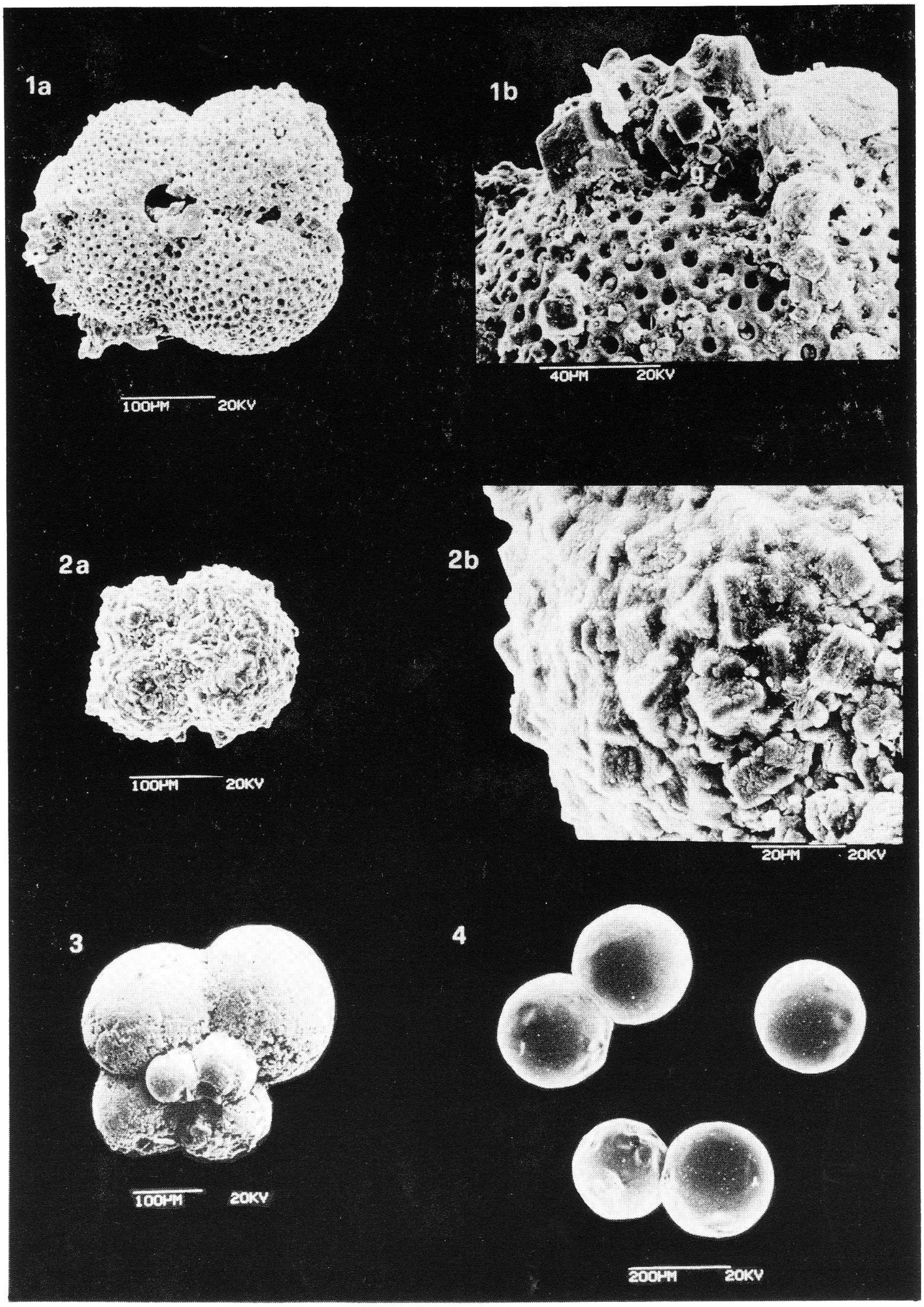
1a
1b
100HM 20KV
40HM 20KV
2a
2b
100HM 20KV
20HM 20KV
3
4
100HM 20KV
200HM 20KV

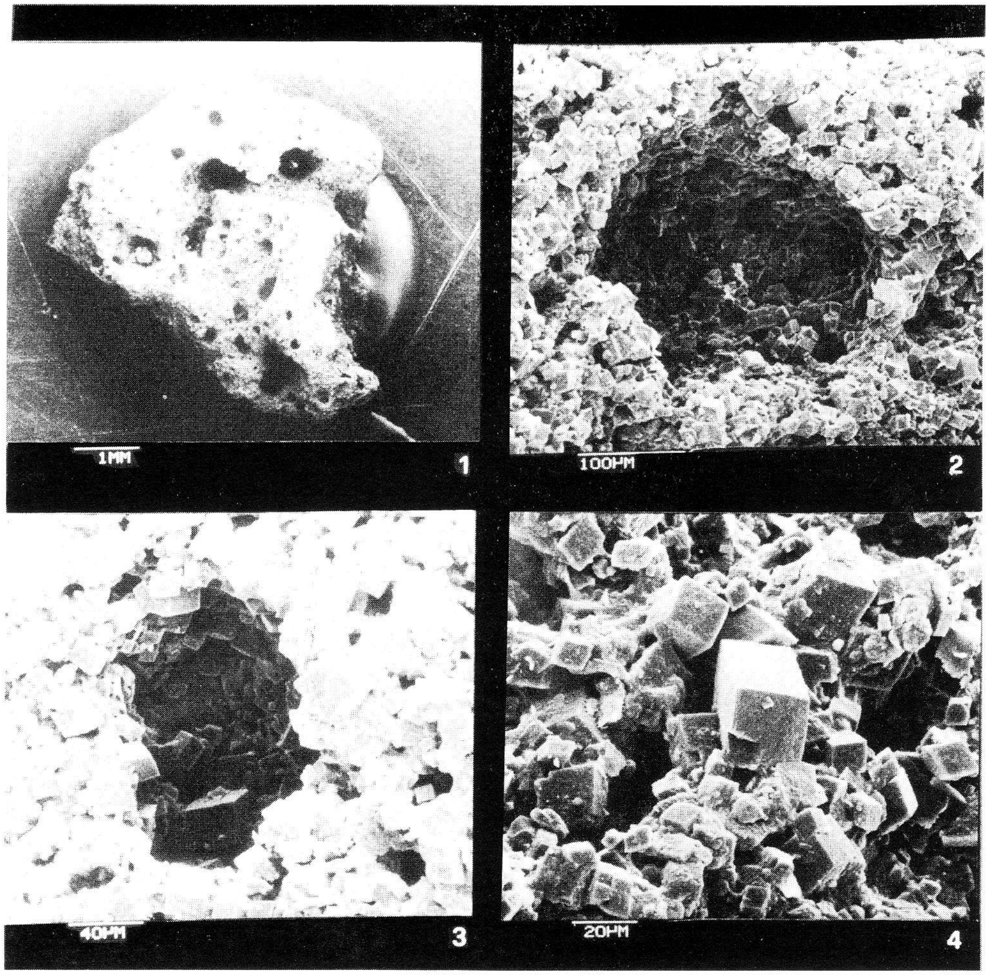
1MM
1
100μM
2
40μM
3
20μM
4